Monthly Notices
of the
ROYAL ASTRONOMICAL SOCIETY

MNRAS **485,** 2–12 (2019) doi:10.1093/mnras/sty3213

Pulse frequency fluctuations of magnetars

D. Çerri-Serim,[1] M. M. Serim,[1] Ş. Şahiner,[1] S. Ç. İnam[2]★ and A. Baykal[1]★

[1]*Physics Department, Middle East Technical University, 06531 Ankara, Turkey*
[2]*Department of Electrical and Electronics Engineering, Başkent University, 06790 Ankara, Turkey*

Accepted 2018 November 23. Received 2018 November 13; in original form 2018 September 23

ABSTRACT

Using *RXTE*, *Chandra*, *XMM–Newton* and *Swift* observations, we construct the power spectra and torque noise strengths of magnetars for the first time. For some of the sources, on time-scales of months to years, we measure strong red noise that might be a consequence of their outbursts. We compare the noise strengths of magnetars with those of radio pulsars by investigating the possible correlations of noise strength with spin-down rate, magnetic field and age. Using these correlations, we find that the noise strengths of magnetars obey similar trends as radio pulsars. However, we do not find any correlation between noise strength and X-ray luminosity, a correlation that has been seen in accretion-powered pulsars. Our findings suggest that the noise behaviour of magnetars resembles that of radio pulsars, but magnetars possess higher noise levels likely because of their stronger magnetic fields.

Key words: stars: magnetars – stars: neutron – pulsars: general.

1 INTRODUCTION

Magnetars are isolated young pulsars that have extremely strong inferred dipolar magnetic fields, which are the strongest among astronomical objects known to date. X-ray observations of magnetars have revealed several interesting observational phenomena, including giant flares, large outbursts, short bursts and quasi-periodic oscillations. Magnetars have also been shown to exhibit distinct timing properties, such as enhanced spin-down, glitches and anti-glitches (see Kaspi & Beloborodov 2017, for a comprehensive review). An accreting system, SXP 1062, has also shown a glitch, with a magnetar field deduced from its spin-down rate (Serim et al. 2017). Using pulse timing techniques, it is possible to detect glitches and anti-glitches, and to study the characteristics of the timing noise of magnetars. Glitches and anti-glitches are the sudden jumps observed in the pulse frequency time series of pulsars, whereas timing noise, which is related to stochastic variations in the time series, is a measure of irregularities in the pulse frequency time series. Timing noise was first discussed for the Crab pulsar (Boynton et al. 1972), and it was found that its noise behaviour corresponds to a random walk in frequency.

Theoretical studies have shown that power density spectra of red noise in timing residuals are generally frequency dependent and proportional to $\sim f^{\alpha}$,where $\alpha = -1$, -3 and -5, corresponding to the timing noise in phase, frequency and spin-down rate, respectively (e.g. D'Alessandro et al. 1995). It is not straightforward to estimate the power density spectra of timing noise because, in general, the data are sampled unevenly over long time-scales ranging from days to years. The idea that timing noise is a type of random walk process is still valid now, but this model is too simple and idealized to explain the noise phenomenon. Cordes & Downs (1985) have presented a detailed model describing timing noise, and they showed that random walk processes were the result of some discrete micro-jumps being superimposed on the timing parameters of the source. Over the years, it has been shown that timing noise is weakly correlated with the period and strongly correlated with the period derivative – implying a strong anticorrelation with characteristic age (Cordes & Helfand 1980; D'Alessandro et al. 1995; Hobbs, Lyne & Kramer 2010).

Until 2010, there were only a few published studies about the calculation of the timing noise of pulsars from longer time-spans of about >10 yr (Shabanova 1995; Baykal et al. 1999; Stairs, Lyne & Shemar 2000; Shabanova, Lyne & Urama 2001). Hobbs et al. (2010) analysed red noise in the timing residuals of 366 pulsars with a time-span of up to 34 yr, concluding that timing noise is weakly correlated with the magnetic field and that timing residuals show a quasi-periodic pattern on long time-scales. In addition, they suggested that the timing noise of pulsars with a characteristic age $<10^5$ yr could be the result of glitch recoveries and that the process that causes slow glitches (i.e. with an increase in frequency but a stable spin-down rate) should not be different from that of timing noise.

In this paper, we present our calculations of the timing noise of all magnetars using the available up-to-date data. To reach our aim, either we reconstruct a given timing solution by phase-connecting the times of arrival, or we use the frequency histories found in the literature (see Table 1 for references). In order to avoid excess noise appearing because of the pulse frequency changes during the glitch events, we exclude time intervals with reported glitch events from

★ E-mail: inam@baskent.edu.tr (SCI); altan@astroa.physics.metu.edu.tr (AB)

Table 1. List of magnetars and their properties.The references cited in the final column are: 1, McGarry et al. (2005); 2, Tiengo, Esposito & Mereghetti (2008); 3, Dib & Kaspi (2014); 4, Rea et al. (2013); 5, Camero et al. (2014); 6, Kulkarni et al. (2003); 7, Güver, Göğüş & Özel (2012); 8, Kuiper et al. (2012); 9, Rodríguez Castillo et al. (2014); 10, Sato et al. (2010); 11, Halpern & Gotthelf (2010); 12, Coti Zelati et al. (2015); 13, Mereghetti et al. (2000); 14, Woods et al. (2002); 15, Kaplan et al. (2002); 16, Mereghetti et al. (2005); 17, Tiengo et al. (2005); 18, Woods et al. (2007); 19, Mereghetti, Esposito & Tiengo (2007); 20, Esposito et al. (2007); 21, Nakagawa et al. (2009); 22, Younes, Kouveliotou & Kaspi (2015); 23, Israel et al. (2003); 24, Gotthelf et al. (2004); 25, Ibrahim et al. (2004); 26, Halpern & Gotthelf (2005); 27, Gotthelf & Halpern (2005); 28, Camilo et al. (2007); 29, Hotan et al. (2007); 30, Bernardini et al. (2009); 31, Camilo et al. (2016); 32, Scholz, Kaspi & Cumming (2014); 33, Esposito et al. (2011); 34, Esposito et al. (2013); 35, Rea et al. (2014); 36, Zhou et al. (2014); 37, Israel et al. (2016).

Source name	P [a] (s)	$\dot{P}$ [a] (10^{-11} s s^{-1})	$B_{\rm surf}$ [a] (10^{14} G)	$L_{\rm x}$ [a] (10^{33} erg s^{-1})	log (S) [b] [log (s^{-3})]	Time-span [b] (d)	Timing param. references
CXOU J010043.1–721134	8.020392(9)	1.88(8)	3.9	65	$-20.47^{+1.19}_{-0.44}$	1881	1, 2 [c]
4U 0142+61	8.68869249(5)	0.2022(4)	1.3	105	$-22.65^{+1.19}_{-0.44}$ **	993	3 [d] (Eph B,C,D)
SGR 0418+5729	9.07838822(5)	0.0004(1)	0.061	0.00096	$-23.68^{+1.19}_{-0.44}$	1865	4 [d]
SGR 0501+4516	5.7620695(1)	0.594(2)	1.9	0.81	$-21.63^{+1.19}_{-0.44}$	547	5 [d]
SGR 0526–66	8.0544(2)	3.8(1)	5.6	189	$-16.91^{+1.19}_{-0.44}$	3543	6, 7 [c]
1E 1048.1–5937	6.457875(3)	2.25	3.9	49	$-18.54^{+0.27}_{-0.18}$	972	3 [e]
1E 1547.0–5408	2.0721255(1)	4.77	3.2	1.3	$-15.56^{+1.19}_{-0.44}$	810	8 [f]
PSR J1622–4950[g]	4.3261(1)	1.7(1)	2.7	0.44	–	–	–
SGR 1627–41[g]	2.594578(6)	1.9(4)	2.2	3.6	–	–	–
CXOU J164710.2–455216	10.610644(17)	<0.04	<0.66	0.45	$-21.66^{+1.19}_{-0.44}$	1066	9 [d]
1RXS J170849.0–400910	11.00502461(17)	1.9455(13)	4.7	42	$-21.71^{+1.19}_{-0.44}$ **	972	3 [d] (Eph C,F)
CXOU J171405.7–381031	3.825352(4)	6.40(5)	5	56	$-16.63^{+1.19}_{-0.44}$	370	10, 11 [c]
SGR J1745–2900	3.76363824(13)	1.385(15)	2.3	<0.11	$-17.70^{+1.19}_{-0.44}$	494	12 [d]
SGR 1806–20	7.54773(2)	49.5	20	163	$-17.33^{+0.27}_{-0.18}$	1063	13–22 [c]
XTE J1810–197	5.5403537(2)	0.777(3)	2.1	0.043	$-19.87^{+0.27}_{-0.18}$	878	23–31 [c]
Swift J1822.3–1606	8.43772106(6)	0.0021(2)	0.14	<0.00040	$-22.60^{+1.19}_{-0.44}$ *	842	32 [d]
SGR 1833–0832	7.5654084(4)	0.35(3)	1.6	–	$-20.52^{+1.19}_{-0.44}$ *	275	33 [d]
Swift J1834.9–0846	2.4823018(1)	0.796(12)	1.4	<0.0084	$-19.60^{+1.19}_{-0.44}$ *	100	34 [d]
1E 1841–045	11.788978(1)	4.092(15)	7	184	$-21.06^{+0.27}_{-0.18}$ **	1016	3 [d] (Eph A,C,E)
3XMM J185246.6+003317	11.55871346(6)	<0.014	<0.41	<0.0060	$-23.62^{+1.19}_{-0.44}$	215	35, 36 [c]
SGR 1900+14	5.19987(7)	9.2(4)	7	90	$-18.19^{+1.19}_{-0.44}$	1058	15, 22 [c]
SGR 1935+2154	3.2450650(1)	1.43(1)	2.2	–	$-20.64^{+1.19}_{-0.44}$	284	37 [d]
1E 2259+586	6.9790427250(15)	0.0483695(63)	0.59	17	$-22.98^{+0.47}_{-0.31}$ **	944	3 [d] (Eph A,B2,D)

Note. [a] and $L_{\rm x}$ values are taken from the McGill Online Magnetar Catalog (Olausen & Kaspi 2014).

[b] Noise levels are measured in this work. The time-span column gives the length of time for the noise measurement.

* and ** show noise measurements previously presented by Serim et al. (2012) and Çerri et al. (2016), respectively.

[c] Timing references are for frequency measurements taken from the literature.

[d] Timing references are for timing solutions used in phase-coherent timing analysis.

[e] Frequencies of 1E 1048.1–5937 are obtained from fig. 5(a) of Dib & Kaspi (2014), and then the light curves are folded at these frequencies.

[f] Frequencies of 1E 1547.0–5408 are obtained from fig. 1(b) of Kuiper et al. (2012), and then the light curves are folded at these frequencies.

[g] The sampling rates of observations are not sufficient to measure the noise strength of these sources.

light curves in the construction of the power density estimation. Out of 23 confirmed magnetars, two are not studied because of the lack of data, and the noise measurements of another three magnetars were already performed in our previous work (Serim, Inam & Baykal 2012). For the remaining 18 sources, either we measure the noise strength or we estimate the power density spectra depending on the sampling rate of the data. The noise strength values are then compared with the noise estimates of radio pulsars. This paper proceeds as follows. In Section 2, we describe the data reduction procedures. In Section 3, we explain the methodology of noise analysis and power density spectra estimation. We report and discuss the results in Section 4.

2 DATA REDUCTION

For this work, we perform the analysis of *XMM–Newton*, *Chandra*, *Swift* and *RXTE* observations of 18 magnetars. We select the data of glitch-free time intervals for our analysis. All data are gathered from the High Energy Astrophysics Science Archive Research Center (HEASARC) archive of the National Aeronautics and Space Administration (NASA).

For *XMM–Newton* observations, data reduction is carried out using SAS v.15.0.0 software. For observations with a high-energy background, we exclude the time intervals in which the background level is higher than 5 per cent of the source flux. Data are filtered for event patterns 0–4 with only good events (FLAG = 0). Source events for all observations are extracted from a 20-arcsec circle centred on the source coordinates. Background events are obtained from a circular source-free region on the same CCD.

Chandra data products are examined using CIAO v.4.9 software. The data are reprocessed to produce the level 2 event files using the REPRO tool of CALDB v.4.7.6. A 5-arcsec circle centred on the source coordinates is used to gather source counts, while a source-free 10-arcsec circle is used to extract background events on the same CCD.

Data reduction of *RXTE* proportional counter array (PCA) data are deployed using HEASOFT v.6.19 software. Data are filtered with the following options: electron contamination to be less than 0.1; elevation angle to be greater than 10; offset angle less than 0.02. From these cleaned event files, light curves with a resolution of 0.05 s are created. The light curves are corrected for PCU on/off status using the CORRECTLC tool within the FTOOLS software.

The *Swift* X-ray telescope (XRT) data are cleaned with the standard pipeline script XRTPIPELINE v.0.13.2 using default screening criteria. Clean event files are barycentred using the source coordinates and an up-to-date clockfile. Light curves are extracted with XSELECT v.2.4D. For windowed timing mode observations, no region selection is applied during light-curve extraction. For photon counting mode observations, a 20-pixel circular source region and a 60-pixel circular background region are used.

3 NOISE AND POWER DENSITY SPECTRA ESTIMATION

If the pulse frequency history of a source has already been presented in the literature, we use the frequencies for noise strength measurements directly (see Table 1, and references therein). If timing ephemerids are presented, then we use the following approach to generate the pulse frequency histories. Using the process described in Section 2, we extract light curves for each source and the time series are corrected for the Solar system barycentre. We employ the phase-coherent timing technique to determine the rotational phase as a function of time $\phi(t)$. A pulse profile for each observation is generated by folding the light curves with the pulse frequency of the source. The template pulse is determined as the one with maximum χ^2 among all pulse profiles. Then, pulse profiles are represented in terms of harmonic functions (Deeter & Boynton 1982) and cross-correlated with the template. As a result of cross-correlation, times of arrival of the pulses (pulse TOAs) are calculated for each observation. The rotational phase of a pulsar as a function of time can be expressed as a Taylor expansion,

$$\Phi(t) = \Phi_0 + \nu(t - t_0) + \frac{1}{2}\dot{\nu}(t - t_0)^2 + \ldots, \quad (1)$$

where ν is the pulse frequency at folding epoch t_0 and $\dot{\nu}$ is the pulse frequency derivative. After constructing pulse TOAs, we split these into many overlapping short time intervals. Each interval contains a different number of pulse TOAs depending on how frequently the source was observed. Then, we fit a linear model pulse TOA within each time interval to measure pulse frequencies. The slope of these linear models, $\delta\phi = \delta\nu(t - t_0)$, allows us to estimate the pulse frequency corresponding to the mid-times of these intervals. Uncertainties in the pulse frequency measurements are obtained using the error range of the slope of the linear model fit within the corresponding time interval, and the horizontal error bars indicate the length of each time interval. The measured pulse frequencies for each source are shown in Fig. 1.

In order to investigate the characteristics of torque noise, we investigated the rms of the residuals of pulse frequency histories for long time-scales and of pulse TOAs for shorter time-scales (if a timing solution was available). The calculated mean square residual value $\langle\sigma_R^2(m, T)\rangle$ depends on the degree m of polynomial removal and the time-span T of the data set. In our analysis, we remove the simple spin-down trend – quadratic model ($m = 2$) for pulse TOAs or linear model ($m = 1$) for pulse frequency histories – for all magnetars. Then, the power density spectra of pulse frequency derivative fluctuations are established by employing the rms residual technique (for details, see Cordes 1980; Deeter 1984). In this technique, the rth-order red noise strength S_r over a time-span T can be estimated by

$$\langle\sigma_R^2(m, T)\rangle = S_r T^{2r-1}\langle\sigma_R^2(m, 1)\rangle_u, \quad (2)$$

where $\langle\sigma_R^2(m, 1)\rangle_u$ is the normalization factor for the unit noise strength. The unit noise strength $\langle\sigma_R^2(m, 1)\rangle_u$ also depends on the degree of the polynomial removed before the calculation of the rms value. This normalization factor for the unit noise strength can be determined by finding the expected mean square residual for unit strength red noise ($S_r = 1$) over a unit time interval ($T = 1$). The normalization factor for the unit noise strength can be obtained either by numerical simulation (Scott, Finger & Wilson 2003) or by direct calculation (Deeter 1984). In our study, we obtained the rth-order noise strength S_r using the normalization factors calculated by Deeter (1984, see tables 1 and 2). If the noise strength estimations are constant, independent of sampling frequency, the power spectra should have a zero slope. In this case, spin frequency fluctuations can be explained with the random walk model and therefore fluctuations of spin frequency derivatives can be expressed as white noise (or delta function fluctuation at the time). Our preliminary analysis shows that the residuals of the spin frequencies can be characterized by first-order red noise (or random walk). The order of red noise ($r = 1, 2, 3, ...$) corresponds to the rth time integral of white noise time series. Therefore, in the construction of power density spectra, we use $r = 1$ for spin frequency histories and $r = 2$ for the pulse TOAs. As a next step, the maximum time-span of the available data set is considered as the longest time-scale (T) and noise strength calculations are repeated for smaller time-scales ($T/2$, $T/4$, ...). The calculated noise strengths on each time-scale are logarithmically averaged and combined into a single power estimate. Finally, the power density spectra of pulse frequency derivative fluctuations are constructed using the power estimates on different time-scales (with the corresponding analysis frequency $f = 1/T$).

4 RESULTS AND DISCUSSION

In this study, we investigate the noise characteristics of magnetars using the power density spectra of pulse frequency derivatives. Power density spectra estimates of 15 magnetars are given in Fig. 2.

Earlier estimates of the power density spectra of SGR 1900+14 and SGR 1806–20 showed steep power density spectra on short time intervals with power-law indices -3.7 ± 0.6 and -3.6 ± 0.7, respectively (Woods et al. 2002). In this study, we construct the power density spectra of SGR 1900+14 and SGR 1806–20 using extended data sets. At shorter time-scales, the steepness of the power density spectra is consistent with the values reported by Woods et al. (2002) but at longer time-scales the power spectra become whiter. Therefore, the overall power-law indices are reduced to -2.61 ± 1.49 and -2.58 ± 0.46 for SGR 1900+14 and SGR 1806–20, respectively. The power density spectra of SGR 1900+14 and SGR 1806–20 are complicated; the power-law index changes for the different frequency ranges analysed.

1E 1048.1–5937 shows red noise behaviour with a power-law index of -1.00 ± 0.22 while SGR J1745–2900 and 1E 1841–045 exhibit ha igh level of timing noise at low frequencies, implying red noise behaviour at long time-scales. However, power estimates at higher frequencies analysed for SGR J1745–2900 and 1E 1841–045 are in agreement with the white noise model in pulse frequency derivatives.

The power density spectra of 1E 2259+586, SGR 0418+5729, SGR 0501+4516, 1RXS J170849.0–400910, SGR 1833–0832 and

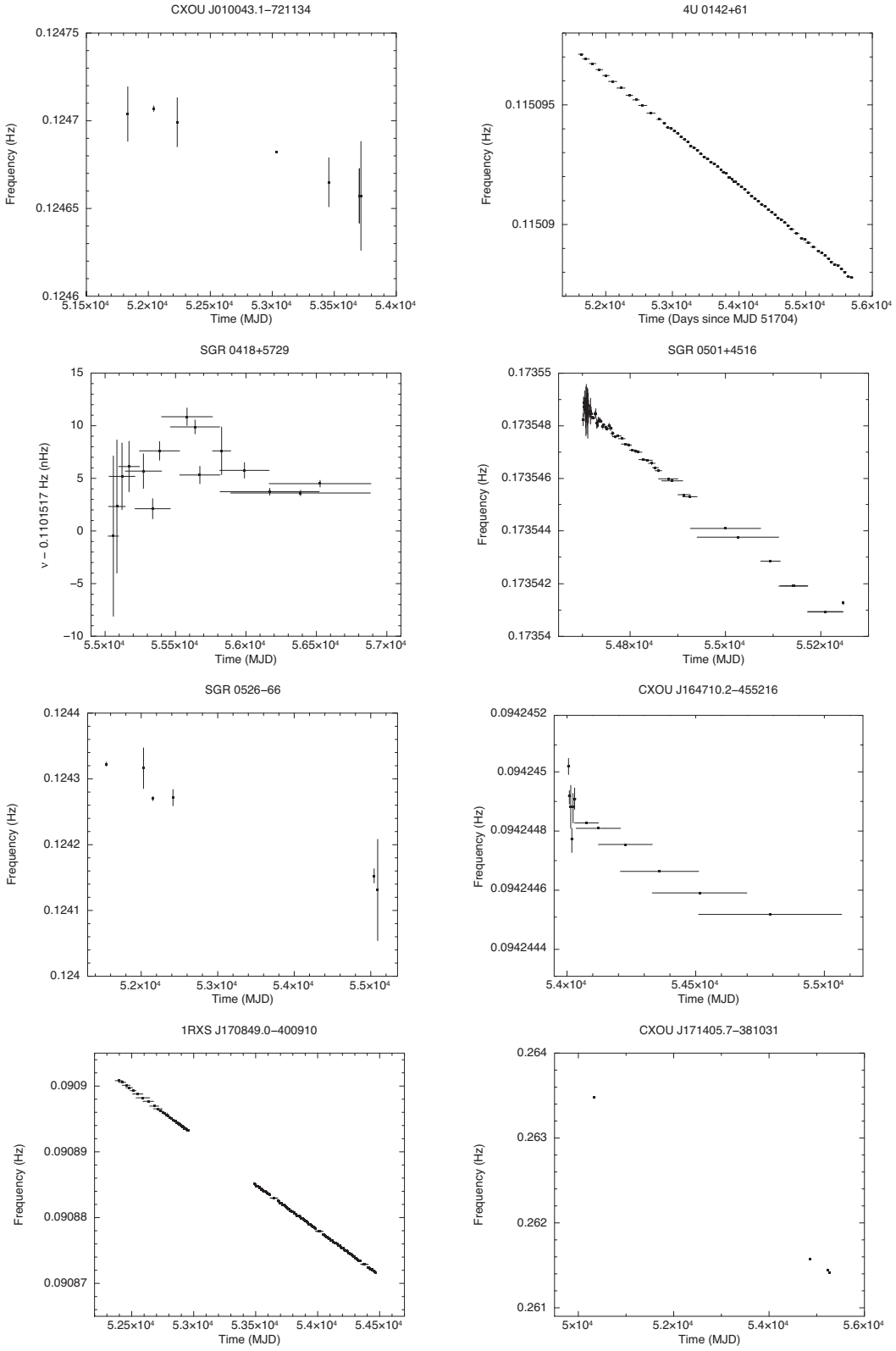

Figure 1. Frequency histories of magnetars. Frequency measurements are taken from the literature for CXOU J010043.1–721134, SGR 0526–66, CXOU J171405.7–381031, SGR 1806–20, XTE J1810–197, 3XMM J185246.6+003317 and SGR 1900+14 (see Table 1 for references). Frequencies of other sources are measured in this work. For two of the sources (SGR 0418+5729 and Swift J1822.3–1606), because their spin-down rates are low, $\Delta\nu$ are plotted instead of ν.

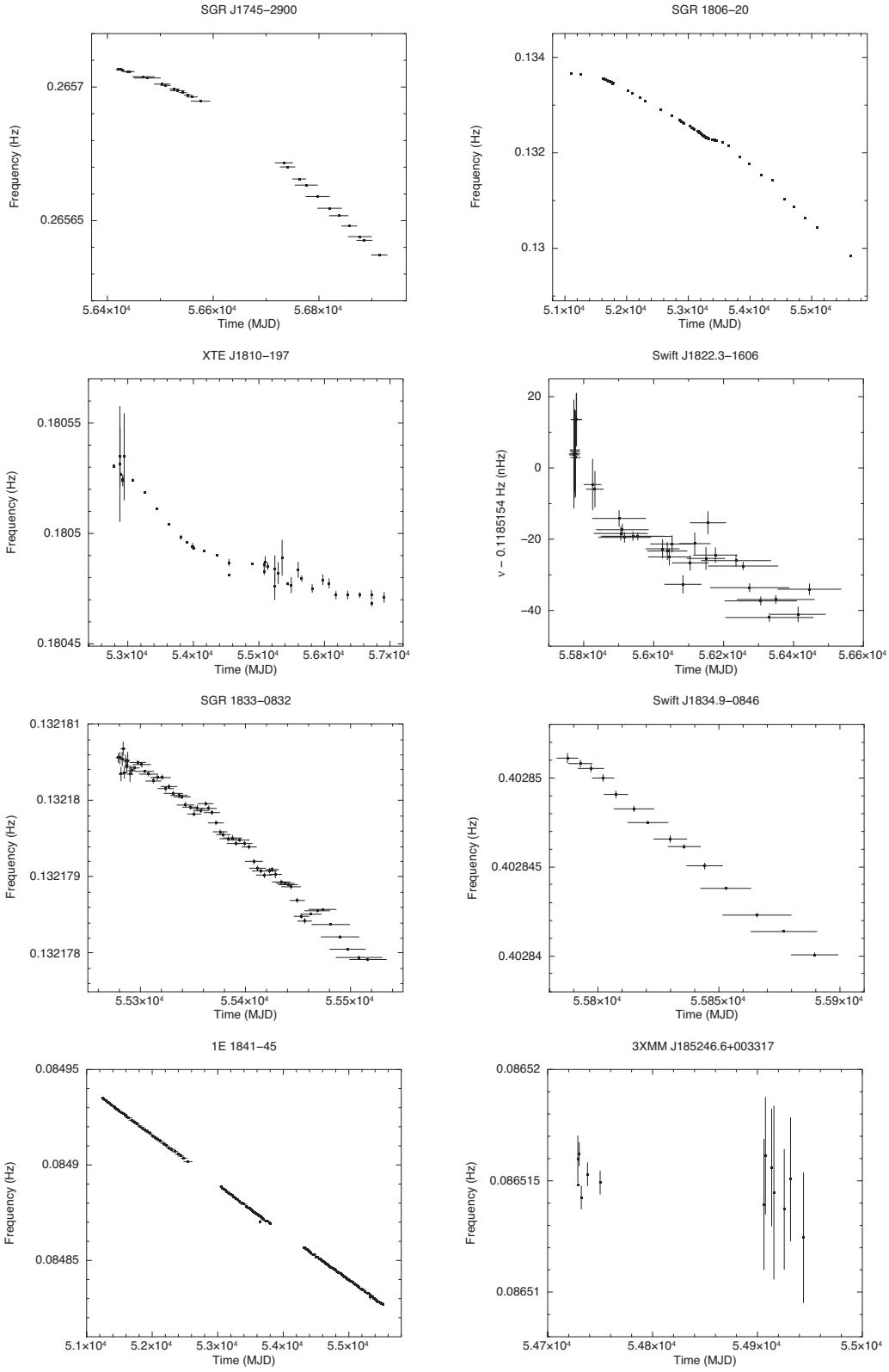

Figure 1. *continued*

XTE J1810–197 track the noise levels of measurements, except for only one or two high power estimates at low frequencies. The power density spectrum of SGR 1935+2154 follows the trend of noise levels in the measurements.

4U 0142+61, 1E 1547.0–5408 and CXO J164710.2–455216 have power-law indices consistent with zero, so the pulse frequency derivative fluctuations are in accord with white noise.

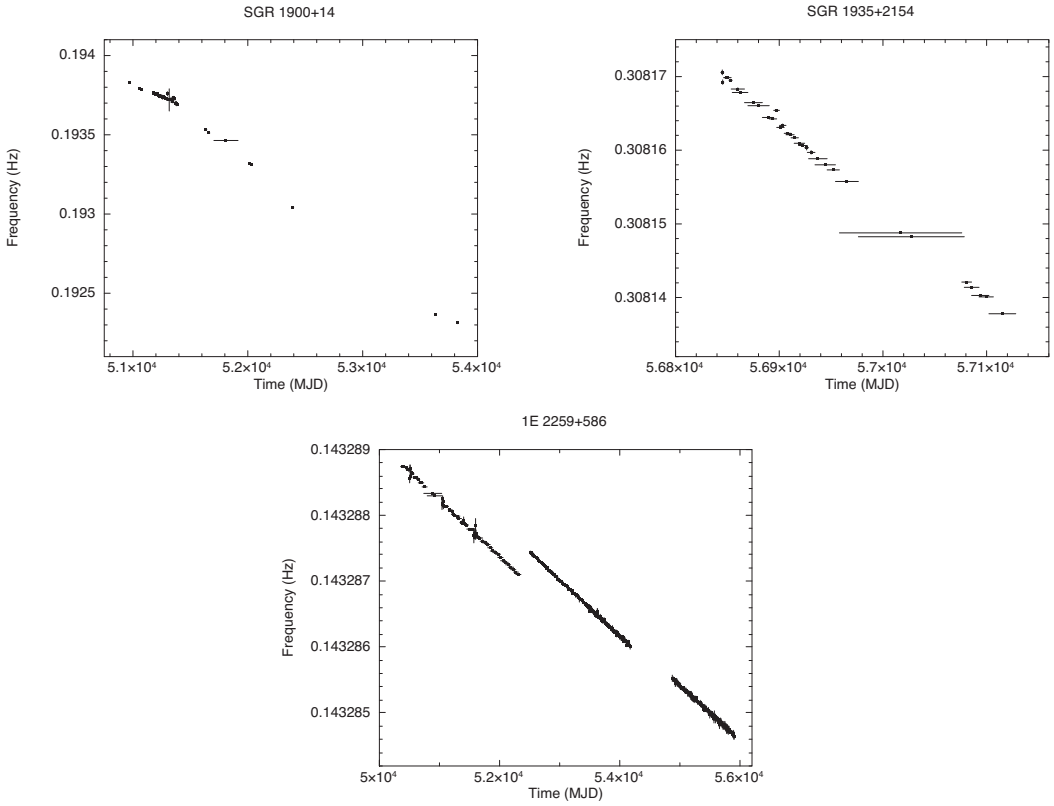

Figure 1. *continued*

For the remaining eight magnetars (CXOU J010043.1–721134, CXOU J171405.7–381031, 3XMM J185246.6+003317, SGR 0526–66, Swift J1822.3–1606, Swift J1834.9–0846, SGR 1627–41 and PSR J1622–4950), the data samplings of spin-frequency measurements are not adequate to construct power density spectra. Therefore, we only measure the timing noise strength of each of these sources using existing data sets.

Recent observations of magnetars mostly take place during outburst activity. In most of the power spectra, we have seen the red noise component at low frequencies, which might be because of the effect of outbursts seen in these sources, such as SGR J1745–2900 (Kaspi et al. 2014), XTE J1810–197 (Camilo et al. 2016) and SGR 1806–20 (Woods et al. 2007; Younes et al. 2015, 2017). The distribution of outbursts might determine the red noise component (i.e. a single outburst might create excess low-frequency noise, or a series of outbursts might create a continuous red noise process). However, the sources 4U 0142+61 and 1E 1547.0–5408 exhibit white noise in power spectra, despite the presence of their outbursts.

1E 1547.0–5408 shows only a marginal excess at the lowest frequency. Following its 2009 outburst, the spin-down rate of 1E 1547.0–5408 recovered its value at 2007 approximately (Dib et al. 2012). Therefore, excess noise appeared only on the longest time-scale (or the lowest frequency), and $\dot{\nu}$ fluctuations at shorter time-spans do not significantly alter the shape of the power spectra. This results in an absence of a red noise component at shorter time-scales.

The bursting behaviour of 4U 0142+61 is similar to that of other magnetars. However, the lack of a red noise component in the power spectra of 4U 0142+61 might also be a consequence of the removal of the previously reported glitch events (see Archibald et al. 2017, and references therein), which are associated with outbursts, in our analysis. Indeed, 4U 0142+61 exhibits quiet timing behaviour between glitch events, compared with other magnetars, and its spin evolution is represented by low-order polynomials (Dib & Kaspi 2014).

Baykal et al. (1999) investigated the stability of second derivatives of spin frequencies of four radio pulsars using the rms residual technique. They suggested that the second derivatives of spin frequencies might originate from red noise processes arising from external torque fluctuations at the magnetosphere of the pulsars (Baykal et al. 1999). The power spectra analysed by Baykal et al. (1999) exhibit red noise with power-law indices varying between –0.39 and –2.41, although they studied only a few systems with long time-spans (of the order of 10 000 d). However, these power spectra are observed to be flat (i.e. consistent with white noise) on shorter time-scales in contrast to some magnetars that show red noise at similar time-scales.

4.1 Noise correlations

To compare the timing noise behaviour of magnetars with radio pulsars, we converted the reported rms values of 366 pulsars (Hobbs et al. 2010) to the noise strength S, using the corresponding normalization factor from table 1 of Deeter (1984). For magnetars, if available, we use the timing noise strength with a time-span of approximately 1 000 d; otherwise, we use the noise strength corresponding to the maximum time-span of the data set (see Table 1). Then, we seek correlations between the noise strength values of magnetars and the other physical parameters such as $\dot{\nu}$, $\dot{P}$, $L_{\rm x}$ and B, as such correlations are observed for pulsars (Cordes 1980; Baykal & Ögelman 1993; Hobbs et al. 2004, 2010). In Fig. 3, we show our results on magnetars, together with the sample set of radio pulsars presented by Hobbs et al. (2010).

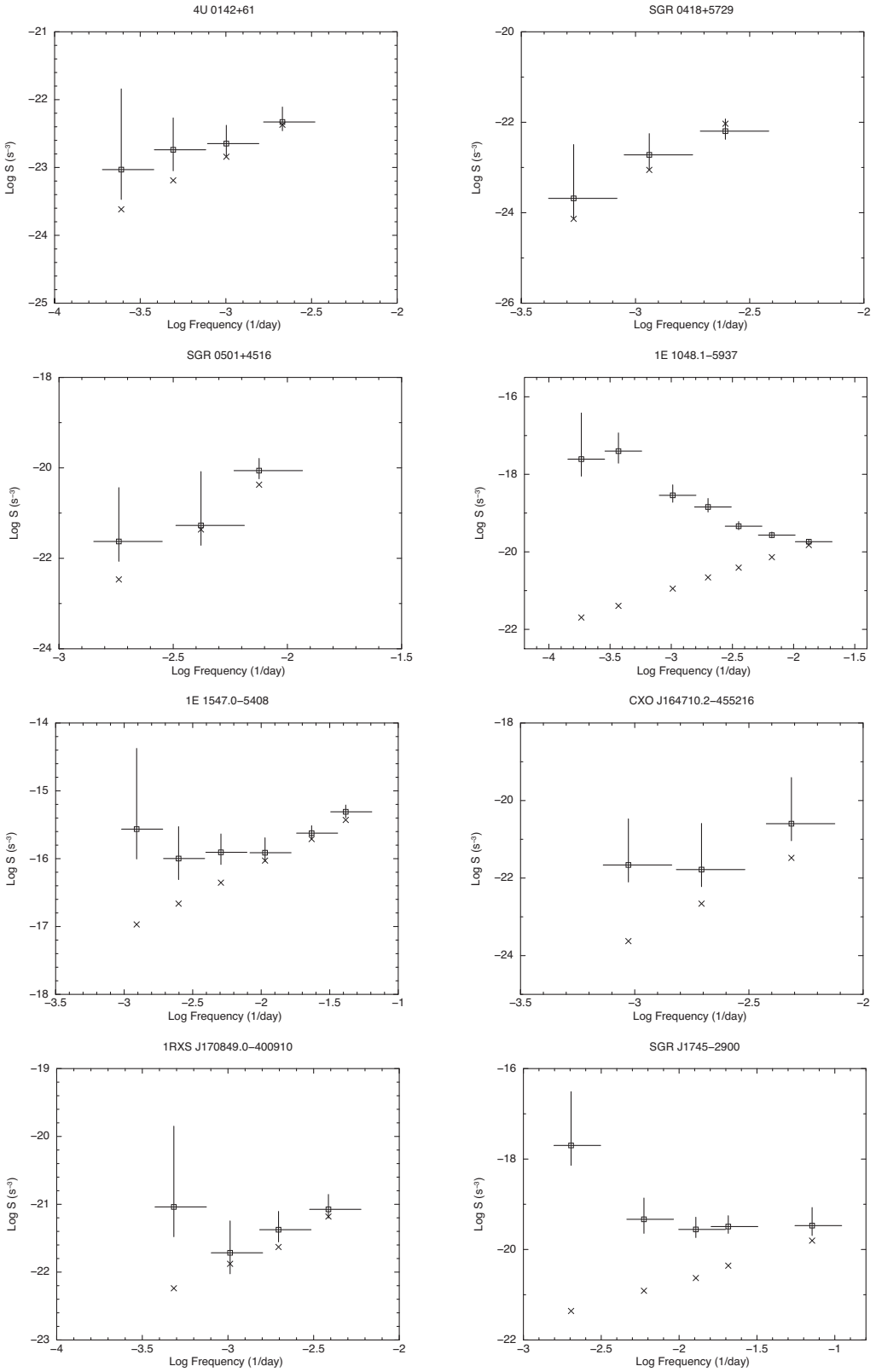

Figure 2. Power density spectra of magnetars. Crosses indicate the power resulting from measurement noise.

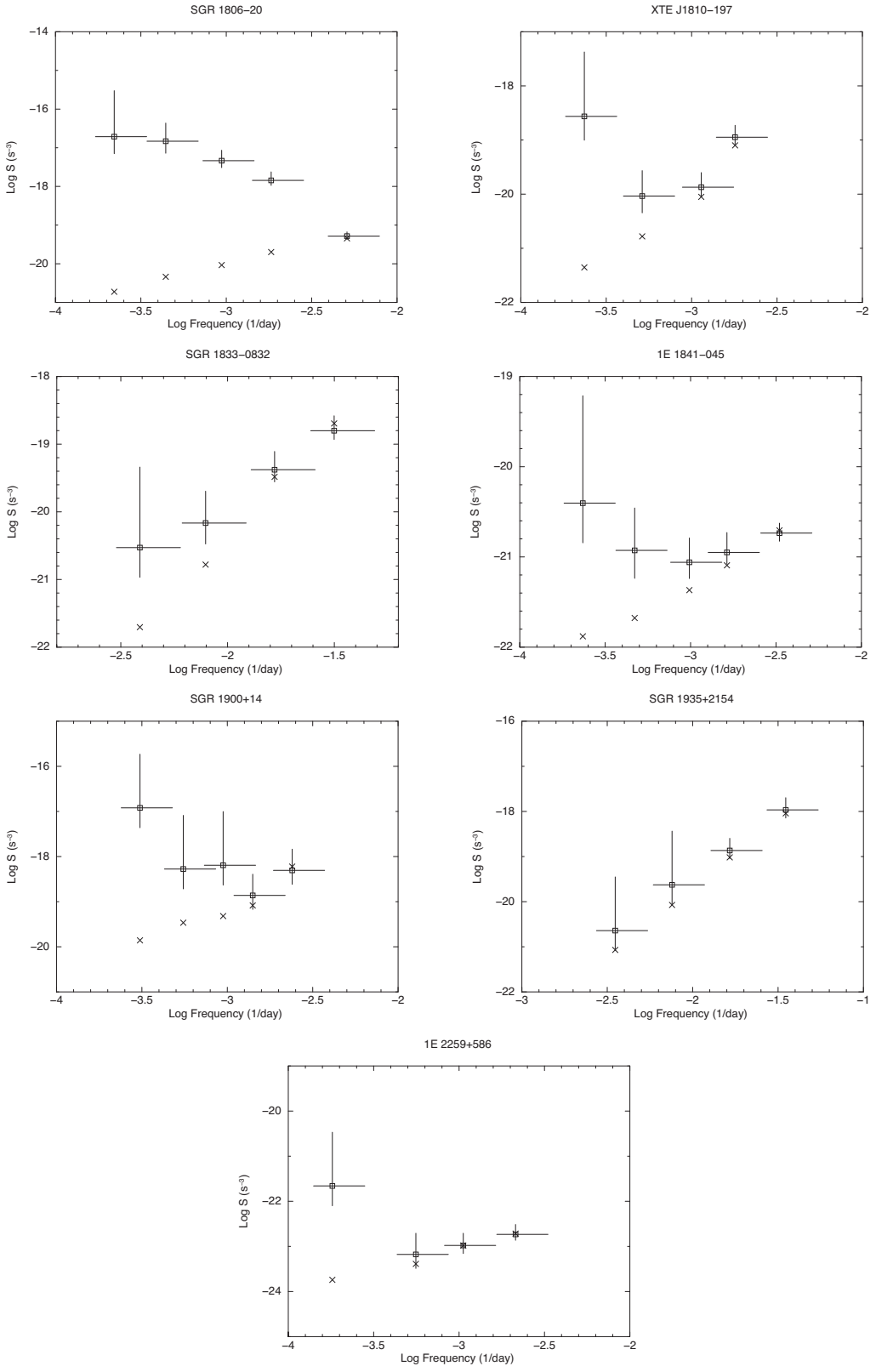

Figure 2. *continued*

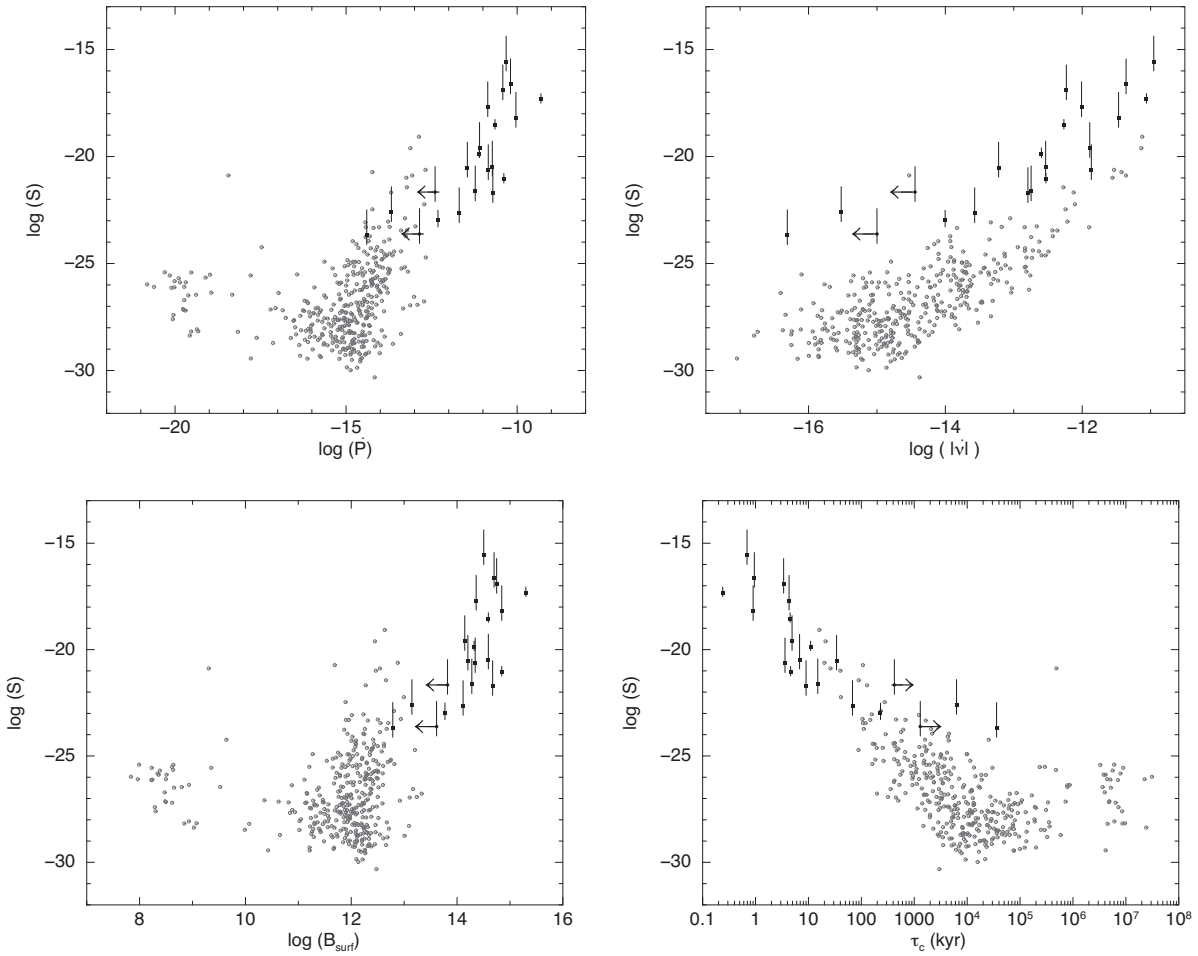

Figure 3. Correlations between noise strength and period derivative (upper-left panel), frequency derivative (upper-right), surface magnetic field strength (lower-left) and characteristic age (lower-right) for magnetars (filled black dots, this work) and radio pulsars (empty grey dots, Hobbs et al. 2010).

In the upper-left panel of Fig. 3, we present noise strength versus period derivative for the sample set of pulsars and magnetars. Our results indicate that there is a correlation between noise strength and $\dot{P}$ for magnetars with a Pearson correlation coefficient of $p = 0.78$. Cordes & Helfand (1980) studied the timing behaviour of 50 pulsars and found that the timing noise of these objects is correlated with their period derivative and uncorrelated with radio luminosity. Our results on magnetars exhibit a correlation analogous to pulsars (Hobbs et al. 2010) and form a continuum with the pulsar population. In the upper-right panel of Fig. 3, a similar type of correlation can also be observed between S and $\dot{\nu}$ ($p = 0.85$, for magnetars only). However, the noise strengths of magnetars seem to be higher than those of the pulsars with the same $\dot{\nu}$, possibly because of either the increased timing activities during magnetar outbursts (Dib & Kaspi 2014) or the noise-dominated $\ddot{\nu}$ values (Baykal et al. 1999). For the first case, increased timing activities during outbursts might explain the higher timing noise levels observed in magnetars, especially when we consider that neutron stars with higher initial magnetic fields ($B > 10^{14}$ G) tend to have more frequent bursting behaviours (Pons & Perna 2011; Perna & Pons 2011). For the latter case, if a pulsar spins down solely as a resut of magnetic braking, the second derivative of the spin frequency should be $\ddot{\nu} = (n\dot{\nu}^2)/\nu$ with the braking index $n = 3$. However, the observed values of braking indices in pulsars vastly differ from the pure dipole braking values, and these vary between –287 986 and +36 246 (Hobbs et al. 2010). Therefore, it is suggested that the observed values of $\ddot{\nu}$ do not originate from pure dipole braking but they are dominated by timing noise (Baykal et al. 1999; Hobbs et al. 2004, 2010).

In the lower-left panel of Fig. 3, we illustrate the noise strengths of the sample set of pulsars and magnetars as a function of their inferred magnetic dipole field strength. Tsang & Gourgouliatos (2013) studied the timing noise behaviour of several AXPs (1E 1841–045, RXS J170849.0–400910, 1E 2259.1+586 and 4U 0142+61) along with a large set of pulsars. They observed a correlation between the frequency noise and magnetic field, which is attributed to the variations in the magnetospheric moment of inertia. We find a similar type of correlation among magnetars with a Pearson correlation coefficient $p = 0.71$. According to the magnetar model, a connection between the timing noise and the B field is expected as most of the physical processes that increase the level of the timing noise (i.e. decay rate and structural changes of the magnetic field, crust cracking, internal stresses and outbursts, etc.) are governed by the strength of the magnetic field (Thompson, Lyutikov & Kulkarni 2002; Pons & Perna 2011; Beloborodov 2009). We also find that there is an anticorrelation between characteristic age τ_c and the timing noise strength of the magnetars (see the lower-right panel of Fig. 3; $p = -0.82$), which is also observed for pulsars (Hobbs et al. 2010). The anticorrelation between τ_c and the noise strength further supports the idea that the timing noise level is decreasing as the magnetic field of the source decays. Considering

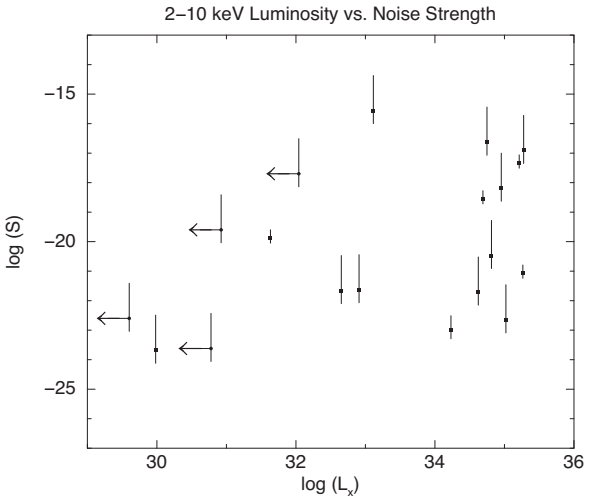

Figure 4. X-ray luminosity versus noise strength of magnetars.

all the correlations, the timing noise strengths of magnetars and pulsars are seem to be linked and they possess a similar noise floor that is possibly associated with their magnetic fields, as suggested by Tsang & Gourgouliatos (2013). A link between these two neutron star populations was also suggested, considering their surface temperatures, quiescent X-ray luminosities, magnetic fields (Kaspi 2010; An et al. 2012) and magnetar-like bursts observed from the high *B*-field pulsars PSR J1119–6127 (Göğüş et al. 2016; Archibald et al. 2017, 2018) and PSR J1846–0258 (Gavriil et al. 2008). Moreover, both the magnetar-like pulsar, PSR J1846–0258 (Ng et al. 2008), and the magnetar, Swift J1834.9–0846 (Younes et al. 2016), are sourrounded by pulsar wind nebulae.

Baykal & Ögelman (1993) studied a set of accreting pulsars, and reported a correlation between X-ray luminosity and timing noise strength. In accreting pulsars, mass transfer episodes enhance X-ray luminosity and exert external torque on the pulsar, implying that the noise strength of accreting pulsars grows with the mass accretion rate. In Fig. 4, we present the noise strength versus the X-ray luminosity of magnetars in which we do not observe any correlation among these parameters ($p = 0.41$). This implies that the fall-back disc model (Alpar 2001), which suggests that the observed X-ray emission and spin-down behaviour of magnetars are sustained by accretion from a debris disc after the supernova explosion, is a less likely explanation for the timing noise of these sources. Therefore, the timing noise of magnetars possibly arises from fluctuations of high dipolar fields, rather than fluctuations of external torque exerted by a debris disc. Together with the results stated above, we conclude that the timing noise behaviour of magnetars forms a continuum with the radio pulsar population, rather than accreting sources.

5 SUMMARY

In this work, we present an extended analysis of the timing noise of all magnetars for the first time. We measure the noise strengths of all magnetars and we construct the power density spectra of 15 magnetars. On the one hand, we see that the noise strength is correlated with the frequency derivative and magnetic field strength, and anticorrelated with age. By comparing these correlations with those found for radio pulsars (Hobbs et al. 2010), we observe that magnetars exhibit a similar timing noise behaviour as radio pulsars. However, magnetars do seem to have higher timing noise levels compared with those of radio pulsars and red noise components arising at shorter time-scales, which are expected as a consequence of the magnetar model (Thompson & Duncan 1995, 1996), as a stronger initial magnetic field leads to increased chances of magnetic structure variations, more frequent bursting behaviour and greater internal stresses (Pons & Perna 2011; Perna & Pons 2011). On the other hand, we do not see a correlation between the noise strength of magnetars and their X-ray luminosity, which was observed for accreting sources (Baykal & Ögelman 1993). Therefore, our findings provide further evidence that magnetar populations are in continuum with radio pulsar populations, as suggested by Kaspi (2010), An et al. (2012) and Tsang & Gourgouliatos (2013). Our results on noise correlations, together with the power density spectra of magnetars, imply that the noise process in magnetars is associated with the magnetospheric moment of inertia fluctuations (Tsang & Gourgouliatos 2013). The noise strengths of magnetars follow the correlations that pulsars show with age and magnetic field. This could imply that the physical processes governing timing noise in both populations are similar, as is independently suggested for glitch events observed in both populations (Dib & Kaspi 2014).

ACKNOWLEDGEMENTS

We acknowledge support from TÜBİTAK, the Scientific and Technological Research Council of Turkey through the research project MFAG 114F345. We are grateful to an anonymous referee for useful comments. AB acknowledges Professor Werner Becker and the Max Planck Institute for Extraterrestrial Physics (MPE) for the invitation to be a guest. The McGill Online Magnetar Catalog can be accessed at http://www.physics.mcgill.ca/˜pulsar/magnetar/main.html.

REFERENCES

Alpar M. A., 2001, ApJ, 554, 1245
An H., Kaspi V. M., Tomsick J. A., Cumming A., Bodaghee A., Gotthelf E. V., Rahoui F., 2012, ApJ, 757, 68
Archibald R. F. et al., 2017, ApJ, 849, L20
Archibald R. F., Kaspi V. M., Tendulkar S. P., Scholz P., 2018, preprint (arXiv:1806.01414)
Baykal A., Ögelman H., 1993, A&A, 267, 119
Baykal A., Ali Alpar M., Boynton P. E., Deeter J. E., 1999, MNRAS, 306, 207
Beloborodov A. M., 2009, ApJ, 703, 1044
Bernardini F. et al., 2009, A&A, 498, 195
Boynton P. E., Groth E. J., Hutchinson D. P., Nanos G. P., Jr, Partridge R. B., Wilkinson D. T., 1972, ApJ, 175, 217
Camero A. et al., 2014, MNRAS, 438, 3291
Camilo F. et al., 2007, ApJ, 663, 497
Camilo F. et al., 2016, ApJ, 820, 110
Çerri D., Serim M. M., Yucalan D., Sahiner S., Inam S. C., Baykal A., van den Heuvel E., 2016, ed, Proc. 11th INTEGRAL Conference, Gamma-Ray Astrophysics in Multi-Wavelength Perspective , PoS(INTEGRAL2016)068
Cordes J. M., 1980, ApJ, 237, 216
Cordes J. M., Downs G. S., 1985, ApJS, 59, 343
Cordes J. M., Helfand D. J., 1980, ApJ, 239, 640
Coti Zelati F. et al., 2015, MNRAS, 449, 2685
D'Alessandro F., McCulloch P. M., Hamilton P. A., Deshpande A. A., 1995, MNRAS, 277, 1033
Deeter J. E., 1984, ApJ, 281, 482
Deeter J. E., Boynton P. E., 1982, ApJ, 261, 337
Dib R., Kaspi V. M., 2014, ApJ, 784, 37
Dib R., Kaspi V. M., Scholz P., Gavriil F. P., 2012, ApJ, 748, 3

Esposito P. et al., 2007, A&A, 476, 321
Esposito P. et al., 2011, MNRAS, 416, 205
Esposito P. et al., 2013, MNRAS, 429, 3123
Gavriil F. P., Gonzalez M. E., Gotthelf E. V., Kaspi V. M., Livingstone M. A., Woods P. M., 2008, Science, 319, 1802
Gotthelf E. V., Halpern J. P., 2005, ApJ, 632, 1075
Gotthelf E. V., Halpern J. P., Buxton M., Bailyn C., 2004, ApJ, 605, 368
Göğüş E. et al., 2016, ApJ, 829, L25
Güver T., Göğüş E., Özel F., 2012, MNRAS, 424, 210
Halpern J. P., Gotthelf E. V., 2005, ApJ, 618, 874
Halpern J. P., Gotthelf E. V., 2010, ApJ, 725, 1384
Hobbs G., Lyne A. G., Kramer M., Martin C. E., Jordan C., 2004, MNRAS, 353, 1311
Hobbs G., Lyne A. G., Kramer M., 2010, MNRAS, 402, 1027
Hotan A. W., Long S. R., Dickey J. M., Dolley T. J., 2007, ApJ, 668, 449
Ibrahim A. I. et al., 2004, ApJ, 609, L21
Israel G. et al., 2003, The Astronomer's Telegram, 203, Available at: http://adsabs.harvard.edu/abs/2003ATel..203....1I
Israel G. L. et al., 2016, MNRAS, 457, 3448
Kaplan D. L., Fox D. W., Kulkarni S. R., Gotthelf E. V., Vasisht G., Frail D. A., 2002, ApJ, 564, 935
Kaspi V. M. et al., 2014, ApJ, 786, 84
Kaspi V. M., 2010, Proceedings of the National Academy of Science, 107, 7147
Kaspi V. M., Beloborodov A. M., 2017, ARA&A, 55, 261
Kuiper L., Hermsen W., den Hartog P. R., Urama J. O., 2012, ApJ, 748, 133
Kulkarni S. R., Kaplan D. L., Marshall H. L., Frail D. A., Murakami T., Yonetoku D., 2003, ApJ, 585, 948
McGarry M. B., Gaensler B. M., Ransom S. M., Kaspi V. M., Veljkovik S., 2005, ApJ, 627, L137
Mereghetti S. et al., 2005, ApJ, 628, 938
Mereghetti S., Cremonesi D., Feroci M., Tavani M., 2000, A&A, 361, 240
Mereghetti S., Esposito P., Tiengo A., 2007, Ap&SS, 308, 13
Nakagawa Y. E. et al., 2009, PASJ, 61, S387
Ng C.-Y., Slane P. O., Gaensler B. M., Hughes J. P., 2008, ApJ, 686, 508
Olausen S. A., Kaspi V. M., 2014, ApJS, 212, 6
Perna R., Pons J. A., 2011, ApJ, 727, L51
Pons J. A., Perna R., 2011, ApJ, 741, 123
Rea N. et al., 2013, ApJ, 770, 65
Rea N., Viganò D., Israel G. L., Pons J. A., Torres D. F., 2014, ApJ, 781, L17
Rodríguez Castillo G. A., Israel G. L., Esposito P., Pons J. A., Rea N., Turolla R., Viganò D., Zane S., 2014, MNRAS, 441, 1305
Sato T., Bamba A., Nakamura R., Ishida M., 2010, PASJ, 62, L33
Scholz P., Kaspi V. M., Cumming A., 2014, ApJ, 786, 62
Scott D. M., Finger M. H., Wilson C. A., 2003, MNRAS, 344, 412
Serim M. M., Inam S. Ç., Baykal A., 2012, in Lewandowski W., Maron O., Kijak J., eds, ASP Conf. Ser. Vol. 466, Electromagnetic Radiation from Pulsars and Magnetars, Astron. Soc. Pac., San Francisco. p. 255
Serim M. M., Şahiner Ş., Çerri-Serim D., Inam S. Ç., Baykal A., 2017, MNRAS, 471, 4982
Shabanova T. V., 1995, ApJ, 453, 779
Shabanova T. V., Lyne A. G., Urama J. O., 2001, ApJ, 552, 321
Stairs I. H., Lyne A. G., Shemar S. L., 2000, Nature, 406, 484
Thompson C., Duncan R. C., 1995, MNRAS, 275, 255
Thompson C., Duncan R. C., 1996, ApJ, 473, 322
Thompson C., Lyutikov M., Kulkarni S. R., 2002, ApJ, 574, 332
Tiengo A., Esposito P., Mereghetti S., Rea N., Stella L., Israel G. L., Turolla R., Zane S., 2005, A&A, 440, L63
Tiengo A., Esposito P., Mereghetti S., 2008, ApJ, 680, L133
Tsang D., Gourgouliatos K. N., 2013, ApJ, 773, L17
Woods P. M., Kouveliotou C., Göğüş E., Finger M. H., Swank J., Markwardt C. B., Hurley K., van der Klis M., 2002, ApJ, 576, 381
Woods P. M., Kouveliotou C., Finger M. H., Göğüş E., Wilson C. A., Patel S. K., Hurley K., Swank J. H., 2007, ApJ, 654, 470
Younes G. et al., 2016, ApJ, 824, 138
Younes G., Kouveliotou C., Kaspi V. M., 2015, ApJ, 809, 165
Younes G., Baring M. G., Kouveliotou C., Harding A., Donovan S., Göğüş E., Kaspi V., Granot J., 2017, ApJ, 851, 17
Zhou P., Chen Y., Li X-D., Safi-Harb S., Mendez M., Terada Y., Sun W., Ge M-Y., 2014, ApJ, 781, L16

This paper has been typeset from a TEX/LATEX file prepared by the author.